Performance analysis of an all-optical OFDM system in presence of non-linear phase noise

Jassim K. Hmood,[1,2] **Sulaiman W. Harun,**[1,3*] **Siamak D. Emami,**[1] **Amin Khodaei,**[3] **Kamarul A. Noordin,**[1] **Harith Ahmad,**[3] **and Hossam M. H. Shalaby**[4,5].

[1]*Faculty of Engineering, University of Malaya, 50603 Kuala Lumpur, Malaysia*
[2]*Laser and Optoelectronic Department, University of Technology, 10066 Baghdad, Iraq*
[3]*Photonics Research Center, University of Malaya, 50603 Kuala Lumpur, Malaysia*
[4]*Department of Electronics and Communications Engineering, Egypt-Japan University of Science and Technology, Alexandria 21934, Egypt*
[5]*Electrical Engineering Department, Alexandria University, Alexandria 21544, Egypt*
[*]*swharun@um.edu.my*

Abstract: The potential for higher spectral efficiency has increased the interest in all-optical orthogonal frequency division multiplexing (OFDM) systems. However, the sensitivity of all-optical OFDM to fiber non-linearity, which causes nonlinear phase noise, is still a major concern. In this paper, an analytical model for estimating the phase noise due to self-phase modulation (SPM), cross-phase modulation (XPM), and four-wave mixing (FWM) in an all-optical OFDM system is presented. The phase noise versus power, distance, and number of subcarriers is evaluated by implementing the mathematical model using Matlab. In order to verify the results, an all-optical OFDM system, that uses coupler-based inverse fast Fourier transform/fast Fourier transform without any nonlinear compensation, is demonstrated by numerical simulation. The system employs 29 subcarriers; each subcarrier is modulated by a 4-QAM or 16-QAM format with a symbol rate of 25 Gsymbol/s. The results indicate that the phase variance due to FWM is dominant over those induced by either SPM or XPM. It is also shown that the minimum phase noise occurs at −3 dBm and −1 dBm for 4-QAM and 16-QAM, respectively. Finally, the error vector magnitude (EVM) versus subcarrier power and symbol rate is quantified using both simulation and the analytical model. It turns out that both EVM results are in good agreement with each other.

OCIS codes: (060.2330) Fiber optics communications; (060.4080) Modulation; (060.4230) Multiplexing; (060.4370) Nonlinear optics, fibers; (060.5060) Phase modulation.

References and links

1. D. Hillerkuss, R. Schmogrow, T. Schellinger, M. Jordan, M. Winter, G. Huber, T. Vallaitis, R. Bonk, P. Kleinow, F. Frey, M. Roeger, S. Koenig, A. Ludwig, A. Marculescu, J. Li, M. Hoh, M. Dreschmann, J. Meyer, S. Ben Ezra, N. Narkiss, B. Nebendahl, F. Parmigiani, P. Petropoulos, B. Resan, A. Oehler, K. Weingarten, T. Ellermeyer, J. Lutz, M. Moeller, M. Huebner, J. Becker, C. Koos, W. Freude, and J. Leuthold, "26 Tbit s-1 line-rate super-channel transmission utilizing all-optical fast Fourier transform processing," Nat. Photonics **5**(6), 364–371 (2011).
2. D. Hillerkuss, M. Winter, M. Teschke, A. Marculescu, J. Li, G. Sigurdsson, K. Worms, S. Ben Ezra, N. Narkiss, W. Freude, and J. Leuthold, "Simple all-optical FFT scheme enabling Tbit/s real-time signal processing," Opt. Express **18**(9), 9324–9340 (2010).
3. S. E. Mirnia, A. Zarei, S. D. Emami, S. W. Harun, H. Arof, H. Ahmad, and H. M. Shalaby, "Proposal and performance evaluation of an efficient RZ-DQPSK modulation scheme in all-optical OFDM transmission systems," J. Opt. Commun. Netw. **5**, 932–944 (2013).
4. J. Armstrong, "OFDM for optical communications," J. Lightwave Technol. **27**(3), 189–204 (2009).
5. W. Shieh, Q. Yang, and Y. Ma, "107 Gb/s coherent optical OFDM transmission over 1000-km SSMF fiber using orthogonal band multiplexing," Opt. Express **16**(9), 6378–6386 (2008).
6. B. J. Dixon, R. D. Pollard, and S. Iezekiel, "Orthogonal frequency-division multiplexing in wireless communication systems with multimode fiber feeds," IEEE Trans. Microw. Theory Tech. **49**(8), 1404–1409 (2001).

7. A. Kim, Y. H. Joo, and Y. Kim, "60 GHz wireless communication systems with radio-over-fiber links for indoor wireless LANs," IEEE Trans. Consumer Electron. 50(2), 517–520 (2004).
8. Y. Ma, Q. Yang, Y. Tang, S. Chen, and W. Shieh, "1-Tb/s single-channel coherent optical OFDM transmission over 600-km SSMF fiber with subwavelength bandwidth access," Opt. Express 17(11), 9421–9427 (2009).
9. R. Schmogrow, M. Winter, B. Nebendahl, D. Hillerkuss, J. Meyer, M. Dreschmann, M. Huebner, J. Becker, C. Koos, and W. Freude, "101.5 Gbit/s real-time OFDM transmitter with 16QAM modulated subcarriers," in *Optical Fiber Communication Conference*(Optical Society of America, 2011), p. OWE5.
10. K. Lee, C. T. Thai, and J.-K. K. Rhee, "All optical discrete Fourier transform processor for 100 Gbps OFDM transmission," Opt. Express 16(6), 4023–4028 (2008).
11. C. C. Wei and J. J. Chen, "Study on dispersion-induced phase noise in an optical OFDM radio-over-fiber system at 60-GHz band," Opt. Express 18(20), 20774–20785 (2010).
12. C.-T. Lin, C.-C. Wei, and M.-I. Chao, "Phase noise suppression of optical OFDM signals in 60-GHz RoF transmission system," Opt. Express 19(11), 10423–10428 (2011).
13. A. J. Lowery, L. B. Du, and J. Armstrong, "Performance of optical OFDM in ultralong-haul WDM lightwave systems," J. Lightwave Technol. 25(1), 131–138 (2007).
14. G. P. Agrawal, *Nonlinear Fiber Optics* (Academic, 2013).
15. Y. Benlachtar, G. Gavioli, V. Mikhailov, and R. I. Killey, "Experimental investigation of SPM in long-haul direct-detection OFDM systems," Opt. Express 16(20), 15477–15482 (2008).
16. X. Zhu and S. Kumar, "Nonlinear phase noise in coherent optical OFDM transmission systems," Opt. Express 18(7), 7347–7360 (2010).
17. A. J. Lowery, S. Wang, and M. Premaratne, "Calculation of power limit due to fiber nonlinearity in optical OFDM systems," Opt. Express 15(20), 13282–13287 (2007).
18. M. Wu and W. I. Way, "Fiber nonlinearity limitations in ultra-dense WDM systems," J. Lightwave Technol. 22(6), 1483–1498 (2004).
19. D. Hillerkuss, T. Schellinger, R. Schmogrow, M. Winter, T. Vallaitis, R. Bonk, A. Marculescu, J. Li, M. Dreschmann, and J. Meyer, "Single source optical OFDM transmitter and optical FFT receiver demonstrated at line rates of 5.4 and 10.8 Tbit/s," in *Optical Fiber Communication Conference*(Optical Society of America, 2010), p. PDPC1.
20. Y. Dou, H. Zhang, and M. Yao, "Generation of flat optical-frequency comb using cascaded intensity and phase modulators," IEEE Photon. Technol. Lett. 24(9), 727–729 (2012).
21. T. Sakamoto, A. Chiba, and T. Kawanishi, "High-bit-rate optical QAM," in *Optical Fiber Communication Conference*(Optical Society of America, 2009), p. OWG5.
22. M. Seimetz, "Performance of coherent optical square-16-QAM-systems based on IQ-transmitters and homodyne receivers with digital phase estimation," in *National Fiber Optic Engineers Conference*(Optical Society of America, 2006), paper NWA4.
23. A. Demir, "Nonlinear phase noise in optical-fiber-communication systems," J. Lightwave Technol. 25(8), 2002–2032 (2007).
24. X. Chen and W. Shieh, "Closed-form expressions for nonlinear transmission performance of densely spaced coherent optical OFDM systems," Opt. Express 18(18), 19039–19054 (2010).
25. S. Reichel and R. Zengerle, "Effects of nonlinear dispersion in EDFA's on optical communication systems," J. Lightwave Technol. 17(7), 1152–1157 (1999).
26. S. Bernard, "Digital communications fundamentals and applications," Prentice Hall, Inc (2001).
27. S. Donati and G. Giuliani, "Noise in an optical amplifier: Formulation of a new semiclassical model," IEEE Journal Quantum Electron 33(9), 1481–1488 (1997).
28. K.-P. Ho and J. M. Kahn, "Electronic compensation technique to mitigate nonlinear phase noise," Lightwave Technology, Journalism 22, 779–783 (2004).
29. A. P. T. Lau, S. Rabbani, and J. M. Kahn, "On the statistics of intrachannel four-wave mixing in phase-modulated optical communication systems," J. Lightwave Technol. 26(14), 2128–2135 (2008).
30. L. Liu, L. Li, Y. Huang, K. Cui, Q. Xiong, F. N. Hauske, C. Xie, and Y. Cai, "Intrachannel nonlinearity compensation by inverse Volterra series transfer function," Lightwave Technology, Journalism 30, 310–316 (2012).
31. J. A. Morgado, D. Fonseca, and A. V. Cartaxo, "Experimental study of coexistence of multi-band OFDM-UWB and OFDM-baseband signals in long-reach PONs using directly modulated lasers," Opt. Express 19(23), 23601–23612 (2011).
32. S. T. Le, K. Blow, and S. Turitsyn, "Power pre-emphasis for suppression of FWM in coherent optical OFDM transmission," Opt. Express 22(6), 7238–7248 (2014).
33. A. Georgiadis, "Gain, phase imbalance, and phase noise effects on error vector magnitude," IEEE Trans. Vehicular Technol. 53(2), 443–449 (2004).

1. Introduction

Due to their promising potentials, all-optical orthogonal frequency division multiplexing (OFDM) techniques have been recently studied for optical transmission system applications [1–3]. All-optical OFDM techniques are much more resilient to dispersion compared to the conventional time-division multiplexing (TDM) techniques [1, 4]. These techniques allow data streams to be transmitted at high-data rates on a large number of subcarriers [5], and are

more spectral efficient in comparison to wavelength-division multiplexing (WDM) techniques [1, 4]. In conventional optical OFDM methods, both inverse fast Fourier transform (IFFT) and fast Fourier transform (FFT) schemes are typically performed in the electronic domain, and therefore have limited bit rates [6–8]. Recently, real-time electronic IFFT/FFT signal processing of 101.5 Gbit/s was demonstrated for OFDM signals [9]. This limitation seems to be the factor that obstructs the generation or reception of terabit per second OFDM signals. An all-optical solution that is capable of reaching beyond the state-of-art electronics speed would therefore be of immense interest [10]. On the other hand, all-optical OFDM techniques significantly suffer from phase noise (PN), which creates a phase rotation term (PRT) on each subcarrier, that causes interference due to the lack of orthogonality of the subcarriers [11–13]. In fiber-optic communication systems, the aforementioned weaknesses of the OFDM might originate from higher sensitivity to fiber nonlinearities, such as self-phase modulation (SPM), cross-phase modulation (XPM), and four-wave mixing (FWM) [14–17]. Therefore, precise calculation of induced nonlinearity, produced by fiber dispersion, is crucial in assessing these purported side effects of OFDM. It has been shown that optical OFDM systems are immune to chromatic dispersion (CD). At high sub-carrier peak power, the total phase noise decreases with CD effects [16].

In this research work, we develop an analytical model that evaluates linear and nonlinear phase noises induced by the interaction of amplified spontaneous emission (ASE) with SPM, XPM, and FWM in both 4-QAM (quadrature-amplitude modulation) and 16-QAM all-optical OFDM transmission systems. In our model, we focus on the phase noise in single polarization. The polarization multiplexing OFDM system adds other significant interferences between the x- and y- polarized signals. It is very important to discuss the phase noise in this system in the future. With this analytical model, we are able to quantify the nonlinear phase noise variation induced by SPM, XPM, and FWM due to variations in sub-carrier peak power, number of subcarriers, fiber length, and channel index.

Our results reveal that, in contrast to WDM optical transmission systems [18] the nonlinear phase noise induced by FWM dominates other factors in all-optical OFDM systems. This phenomenon is likely due to the subcarriers of all-optical OFDM systems modulated from optical frequency combs, where the interaction is derived from the same laser source. Furthermore, the spacing between subcarriers is equal to the symbol rate. The effects of fiber chromatic dispersion (CD) on the total phase noise in all-optical OFDM systems are studied as well.

The accuracy of our analytical model is verified by quantifying the error vector magnitude (EVM) using both numerical simulation (using VPItransmissionMaker[®] commercial software) and the analytical model. It turns out that both EVM results are in good agreement with each other. The rest of the paper is organized as follows. The proposed transmitter and receiver setup is presented in Section 2. Section 3 is devoted for the analytical modeling of all-optical OFDM system. The analytical and simulation results are presented in Section 4, where the impacts of fiber dispersion, number of subcarriers, fiber length, and subcarrier peak power on the variance of the total phase noise are studied. The validation of our analytical model using simulation results of our systems is presented in the same section as well. Finally, conclusion is given in Section 5.

2. All-optical OFDM system

In this section, we describe our all-optical OFDM system model including both the transmitter and receiver.

2.1. All-optical OFDM transmitter

The transmitter side of the all-optical OFDM transmission system is shown in Fig. 1 [1, 19]. The transmitter consists of an optical frequency comb generator (OFCG), wavelength selected switch, optical QAM modulators, and an optical beam combiner. The OFCG part utilizes an intensity modulator (IM) and two phase modulators (PMs) driven directly by a sinusoidal waveform [20]. In the OFCG scheme, the flatness of OFCG is affected by the ratio of a DC

bias to half-wave voltage of the intensity modulator and the phase shifts between the sinusoidal waveforms applied to the intensity and phase modulators, as depicted in Fig. 1. By setting appropriate values, a 29 flat top comb frequency lines, with frequency spacing of Δf = 25 GHz, can be generated. Subsequently, the wavelength selection switch splits the odd and even subcarriers. The subcarriers are individually modulated with two optical QAM modulators [1, 19]. As shown in Fig. 1, an optical QAM modulation signal is generated from an IQ modulator comprising two Mach Zehnder modulators (MZMs) with two orthogonal components. The in-phase component of the intricate envelope modulates the optical carrier within the upper arm, while the quadrature phase component modulates the 90° stage shifted optical carrier in the lower arm [21, 22]. The QAM encoder is supplied by two independent branches of pseudo-random binary sequence (PRBS) signals, each has a length of $2^{11} - 1$. To preserve the orthogonality of the OFDM signals, the OFDM symbol duration is set to $T_s = 1/\Delta f$ [2].
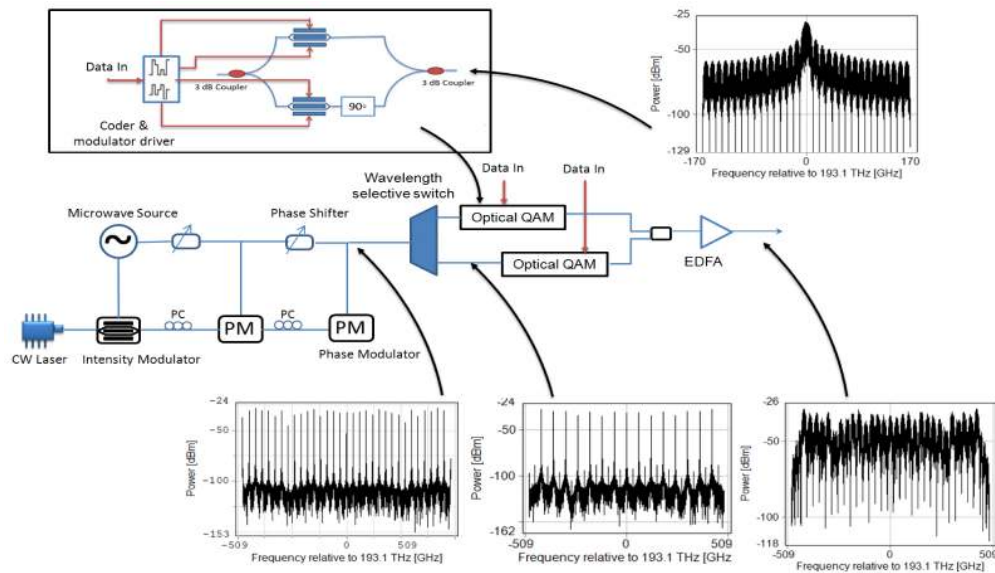

Fig. 1. Transmitter of an all-optical OFDM transmission system.

2.2. All-optical OFDM receiver

The schematic diagram of an all-optical OFDM receiver is shown in Fig. 2. The received OFDM signal is processed using a low-complexity all-optical FFT (OFFT) circuit, which has been proposed by [1, 2]. Our setup is composed of 4-order OFFT to perform both serial-to-parallel conversions and FFT in the optical domain using 3-cascaded Mach-Zehnder Interferometers (MZIs), with subsequent time gates and optical phase modulators. The first MZI time delay is adjusted to $T_s/2$, while the time delays of the other two subsequent parallel MZIs are set to $T_s/4$. After being processed by the OFFT, the resulting signals are sampled by electro-absorption modulators (EAMs). The output from each EAM is fed to an optical fourth-order super Gaussian band-pass filter and is detected using a QAM demodulator. The bit error rates of the resulting signals are measured using a bit-error rate tester (BERT).

3. Analytical modeling of an all-optical OFDM system

In this section, we provide an analytical model that describes the nonlinear interaction between ASE noise and the nonlinear effects in all-optical OFDM with and without dispersion. Nonlinear effects have been reported to be significant in amplified WDM transmission systems [18]. Phase degradation due to SPM, XPM, and FWM has been studied extensively with and without dispersion [23]. It has been shown that ASE due to optical

amplifiers adds a random nonlinear phase noise and mainly affects SPM, XPM, and FWM phenomena [16]. The optical dispersion-management has significant effect on the phase noise. The residual dispersion over multi-spans fiber causes a phase array effect [24]. In our model, the dispersion compensation ratio is assumed to be one and there is no residual dispersion. We start with the following optical system model [18]:
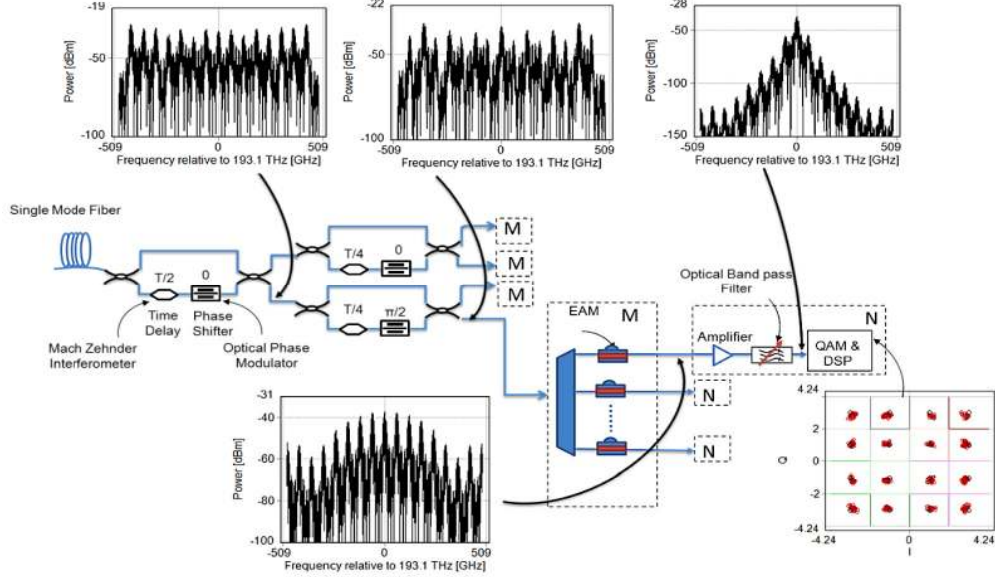
$$u(z,t) = \left[u_k(0,t) + n(t) \right] \exp(j\phi), \tag{1}$$

Fig. 2. Receiver components of an all-optical OFDM transmission system with all-optical FFT scheme.

where $u(0, t)$ and $u(z, t)$ are transmitted and received optical OFDM signals, respectively, z is the transmission distance, $n(t)$ is the ASE noise due to the optical amplifier, and ϕ is phase distortion in radians due to the nonlinearities and dispersion, given by:

$$\phi = \phi_{DIS} + \phi_{SPM} + \phi_{XPM} + \phi_{FWM} + \phi_{SPM}^n + \phi_{XPM}^n + \phi_{FWM}^n + \phi_{FWM}^n, \tag{2}$$

where ϕ_{DIS}, ϕ_{SPM}, ϕ_{XPM}, and ϕ_{FWM} denote the phase distortions due to dispersion, SPM, XPM, and FWM phenomena, respectively. $\phi_{SPM}^n, \phi_{XPM}^n$, and ϕ_{FWM}^n also denote the phase distortions due to interaction of SPM, XPM, and FWM with ASE noise, respectively. The optical field of the all-optical OFDM signal can be written as:

$$u(z,t) = \sum_{k=-(N-1)/2}^{(N-1)/2} u_k(z,t) \exp(j\omega_k t), \tag{3}$$

where N represents the total number of subcarriers (assumed odd without loss of generality), $\omega_k = 2\pi k / T_s$ is the frequency offset from the reference optical carrier, $u(z,t)$, $k \in \{-(N-1)/2, -(N-1)/2+1, \dots, (N-1)/2\}$ is normalized slowly varying field envelope of a single QAM subcarrier. At the transmitter side, it is given by:

$$u(0,t) = \sqrt{\frac{P}{2}} \left(a_k + jb_k \right) rect\left(\frac{t - kT_s}{T_s} \right), \tag{4}$$

where P is the lowest subcarrier optical power, and

$$rect(t) = \begin{cases} 1; & if \ 0 \leq t < 1, \\ 0; & Otherwise. \end{cases} \tag{5}$$

Notice that the complex amplitude is given by $A_k = a_k + jb_k$, for any natural number k, and is dependent on the QAM constellation.

3.1. SPM and XPM phase noise in all-optical OFDM systems

In this subsection, we derive analytical equations for nonlinear phase noise variations of both SPM and XPM phenomena in our all-optical OFDM system, including the interaction of ASE noise. The first consequence of the Kerr effect is SPM, where the optical field experiences a nonlinear phase delay that results from its own intensity. On the other hand, XPM refers to the nonlinear phase shift of an optical field induced by another field with different wavelength, direction, or state of polarization. The optical OFDM signal is commonly transmitted through multi-span optical fiber where each span is composed of an optical fiber and an optical amplifier. At the output of each amplifier, an ASE noise field is added to each subcarrier, which is appropriately modeled as an additive white Gaussian noise [25]. The mean noise energy per degrees of freedom (DOF) is equal to the total noise energy in overall bandwidth and time divided by the number of DOFs [26, 27]. In our analytical model, each fiber span has the same length L and identical optical amplifier with ASE noise $n(t)$. Let us expand the noise field as a discrete Fourier transform:

$$n(t) = \sum_{k=-(N-1)/2}^{(N-1)/2} n_k(t) \exp(j\omega_k t), \tag{6}$$

where $n(t)$, $k \in \{-(N-1)/2, -(N-1)/2+1, \ldots, (N-1)/2\}$, is the complex amplifier noise at the kth subcarrier which have noise variance of σ_k^2. As previously explained, the all-optical OFDM signal is transmitted over M fiber spans. The optical signal is periodically amplified by optical amplifiers located at the end of each span, so the nonlinear phase noise is accumulated span-by-span [28]. In an all-optical OFDM link with M optical amplifiers, the phase noise due to SPM and XPM can be expressed as:

$$\phi_{kSPM}^{n+}(ML) = \gamma L_{eff}(L) \sum_{m=1}^{M} \left| u_k(0,t) + \sum_{\mu=1}^{m} n_{k\mu}(t) \right|^2$$

$$\phi_{kXPM}^{n+}(ML) = 2\gamma L_{eff}(L) \sum_{\substack{i=-(N-1)/2 \\ i \neq k}}^{(N-1)/2} \sum_{m=1}^{M} \left| u_i(0,t) + \sum_{\mu=1}^{m} n_{i\mu}(t) \right|^2, \tag{7}$$

respectively, where γ is the nonlinear coefficients and $n_{k\mu}(t)$, $\mu \in \{1, 2, \ldots, M\}$, is the complex amplifier noise at the μth span and kth subcarrier. Here, $L_{eff} = (1 - e^{-\alpha L})/\alpha$, where α is the attenuation coefficient. Expanding the right-hand sides of the last two equations, we get:

$$\phi_{kSPM}^{n+}(ML) = \gamma L_{eff}(L)\sum_{m=1}^{M}\left[|u_k|^2 + 2\Re\left\{u_k\sum_{\mu=1}^{m}n_{k\mu}^*(t)\right\} + \left|\sum_{\mu=1}^{m}n_{k\mu}(t)\right|^2\right]$$

$$\phi_{kXPM}^{n+}(ML) = 2\gamma L_{eff}(L)\sum_{\substack{i=-(N-1)/2\\i\neq k}}^{(N-1)/2}\sum_{m=1}^{M}\left[|u_i|^2 + 2\Re\left\{u_i\sum_{\mu=1}^{m}n_{i\mu}^*(t)\right\} + \left|\sum_{\mu=1}^{m}n_{i\mu}(t)\right|^2\right], \tag{8}$$

respectively, where $\Re\{x\}$ and x^* denote the real part and the conjugate of complex number x, respectively. The last terms on the right-hand side of Eq. (8) represents the interaction of noise with itself, which has no effect on phase noise, while the first and second terms represent the interaction of the signal with itself and with ASE noise, respectively. The SPM and XPM phase noises due to the interaction of the signal with itself are:

$$\phi_{kSPM}(ML) = \gamma L_{eff}(L)\sum_{m=1}^{M}|u_k|^2$$

$$\phi_{kXPM}(ML) = 2\gamma L_{eff}(L)\sum_{\substack{i=-(N-1)/2\\i\neq k}}^{(N-1)/2}\sum_{m=1}^{M}|u_i|^2, \tag{9}$$

The corresponding terms due to interaction of the signal with ASE noise are:

$$\phi_{kSPM}^{n}(ML) = 2\gamma L_{eff}(L)\sum_{m=1}^{M}\Re\left\{u_k\sum_{\mu=1}^{m}n_{k\mu}^*(t)\right\}$$

$$\phi_{kXPM}^{n}(ML) = 4\gamma L_{eff}(L)\sum_{\substack{i=-(N-1)/2\\i\neq k}}^{(N-1)/2}\sum_{m=1}^{M}\Re\left\{u_i\sum_{\mu=1}^{m}n_{i\mu}^*(t)\right\}, \tag{10}$$

For an OFDM system employing QAM modulation, $u_k \in \left\{\sqrt{P/2}A_k\right\}$. The nonlinear phase noise variances due to interaction SPM and XPM with ASE can be written as:

$$\sigma_{kSPM}^2(ML) = \frac{M(M+1)}{2}\gamma^2 L_{eff}^2(L)P|A_k|^2\sigma_k^2$$

$$\sigma_{kXPM}^2(ML) = 2M(M+1)\gamma^2 L_{eff}^2(L)P\sum_{\substack{i=-(N-1)/2\\i\neq k}}^{(N-1)/2}|A_i|^2\sigma_i^2 \tag{11}$$

It is clear that the phase noise variance due to XPM is much higher than the phase noise variance due to SPM.

3.2. FWM phase noise

In this section, the effect of FWM on all-optical OFDM is analytically demonstrated. As FWM is a phase sensitive process (the interaction depends on the relative phases of all subcarriers), its effect can efficiently accumulate over longer distances. Also, the interaction of FWM with the ASE noise inside the optical fiber is analytically presented. The interaction between FWM and random noise of optical amplifier leads to deterministic as well as stochastic impairments. By including ASE noise and FWM with the other nonlinear and dispersion effects, the optical field of signal at the end of first span can be expressed by [29]:

$$u_k(L,t) = u_k(0,t)\exp\left[j\phi_{kSPM}(L) + j\phi_{kXPM}(L) + j\phi_{kSPM}^{n}(L) + j\phi_{kXPM}^{n}(L) - j\phi_{DIS}(L)\right] + n_k(t) + \delta u_k^n(L,t), \tag{12}$$

where

$$\phi_{DIS}(L) = -\left(\frac{\beta_2}{2}\omega_k^2\right)L$$

$$\delta u_k^n(L,t) = j2\gamma \sum_{\substack{h=-(N-1)/2 \\ h \neq k}}^{(N-1)/2} \sum_{\substack{i=-(N-1)/2 \\ l=h+i-k \\ i \neq l}}^{(N-1)/2} L_{FWM}(L)\left[u_h(L,t)+n_h(t)\right]\left[u_i(L,t)+n_i(t)\right]\left[u_l^*(L,t)+n_l^*(t)\right]$$

(13)

$$L_{FWM}(L) = \frac{1-\exp\left[-L\left(\alpha - j\frac{\beta_2}{2}\Omega^2\right)\right]}{\alpha - j\frac{\beta_2}{2}\Omega^2}$$

$$\Omega^2 = (h^2 + i^2 - l^2 - k^2)\omega^2$$

and β_2 is the dispersion profile. We can define $\frac{\beta_2}{2}\Omega^2 z$ as a phase mismatched between subcarriers. We can rewrite Eq. (12) as:

$$u_k^n(L,t) = u_k(L,t) + \Delta u_k^n(L,t), \tag{14}$$

The fluctuation of the optical field due to both ASE noise and its interaction with FWM for *M* amplifiers (*M* fiber spans) is determined by $\Delta u_k^n(L,t)$ and can be expressed as:

$$\Delta u_k^n(ML,t) = \sum_{m=1}^{M} n_{km} + j2\gamma \sum_{m=1}^{M} \sum_{\substack{h=-(N-1)/2 \\ h \neq k}}^{(N-1)/2} \sum_{\substack{i=-(N-1)/2 \\ l=h+i-k \\ i \neq l}}^{(N-1)/2} L_{FWM}(mL)\left(u_h u_i n_l^* + u_h u_l^* n_i + u_i u_l^* n_h\right) \tag{15}$$

In order to calculate the phase noise variance, the deviation of all-optical OFDM field is considered. The phase noise is defined as:

$$\phi_{kFWM}^n(ML,t) \cong \frac{\Im\left\{\Delta u_k^n(ML,t)\right\}}{|u_k|}, \tag{16}$$

where $\Im\{x\}$ denote the imaginary part of *x*. By substituting the deviation of all-optical OFDM field in Eq. (16), the phase noise variance can be expressed by:

$$\sigma_{kFWM}^2(ML,t) = \frac{2M\sigma_k^2}{P|A_k|^2} + \frac{2\gamma^2 P}{|A_k|^2} \sum_{m=1}^{M} \sum_{\substack{h=-(N-1)/2 \\ h \neq k}}^{(N-1)/2} \sum_{\substack{i=-(N-1)/2 \\ l=h+i-k \\ i \neq l}}^{(N-1)/2} L_{FWM}(mL)$$

$$\times\left(|A_h|^2 |A_i|^2 \sigma_l^2 + |A_h|^2 |A_l|^2 \sigma_i^2 + |A_i|^2 |A_l|^2 \sigma_h^2\right) \tag{17}$$

In the last equation, the first term represents the phase variance due to ASE noise of M optical amplifiers, while the second term expresses the phase noise variance due to the interaction of FWM with ASE noise. From Eq. (11) and Eq. (17), we can conclude that the phase variance due to FWM is dominant over those induced by either SPM or XPM.

4. Results and discussions

In this section, we evaluate our analytical model numerically based on the system described in Section 2. Next, the analytical results of the all-optical OFDM system is demonstrated and compared with numerical simulation results.

4.1. Analytical results

In this subsection, the effects of phase noise on the reception of all-optical OFDM 4- and 16-QAM signals are studied. The influences of subcarrier peak power, number of sub-carriers, fiber length, and symbol rate, on the phase variation are examined as well. In our evaluations, we use a standard single-mode fiber (SSMF) with the following parameters: dispersion of 16 ps/nm/km, attenuation coefficient of 0.2 dB/km, core effective area of $A_{eff} = 80\mu m^2$, and nonlinear refractive index of $n_2 = 2.5 \times 10^{-20}$ m^2/W. In order to compensate for the attenuation, optical amplifiers are employed at spans of 55 km spacing, each. The typical value of the noise figure depends on the manufacture of the optical amplifier. For this reason, in many publications the noise figure is set around 4.5 dB − 5 dB, while others fix the noise figure around 5 dB − 6 dB [30, 31]. In the simulation, the noise figure of each optical amplifier is set to 6 dB for testing the proposed system at higher ASE noise. Furthermore, the dispersion is fully compensated by using a dispersion compensating fiber (DCF) at end of each span.

4.1.1. Phase noise variance versus sub-carrier peak power

Figure 3(a) shows the variance of total nonlinear phase noise as a function of the launch power for a 4-QAM all-optical OFDM system. The fiber length and the number of subcarriers are fixed at 550 km (10 spans) and 29 subcarriers, respectively. The analytical results are evaluated at two dispersion values, namely D = 0 ps/nm/km and D = 16 ps/nm/km, respectively. It is clear that the degradation due to nonlinearity is significantly compensated by the chromatic dispersion effect, whereby phase mismatch (that is related to dispersion) would correspond to a significant decrease in the nonlinear phase variance, cf. Equation (13). The total variance of the phase noise initially decreases with the increase of launch power since the phase noise due to the interaction of ASE noise is dominant at low launch powers. However, as the launch power increases beyond −7 dBm, the variance of phase noise increases dramatically at D = 0 ps/nm/km, since the nonlinear phase noise due to the interaction of XPM and FWM with ASE noise becomes dominant at higher powers. As shown in Fig. 3(b), the interaction of FWM with ASE noise has a major contribution to phase noise in the system. This phenomenon is because the interaction is dependent on the relative phases of all subcarriers in FWM. Similarly, when increasing the dispersion to D = 16 ps/nm/km, the variance of FWM phase noise decreases as the subcarrier power increases until the subcarrier power reaches −3 dBm, beyond which the variance of the phase noise starts to increase. That is, for 4-QAM all-optical OFDM system, a minimum phase noise variance of 0.0108 rad^2 is achieved at an optimum power of −3 dBm as shown at Fig. 3(a).
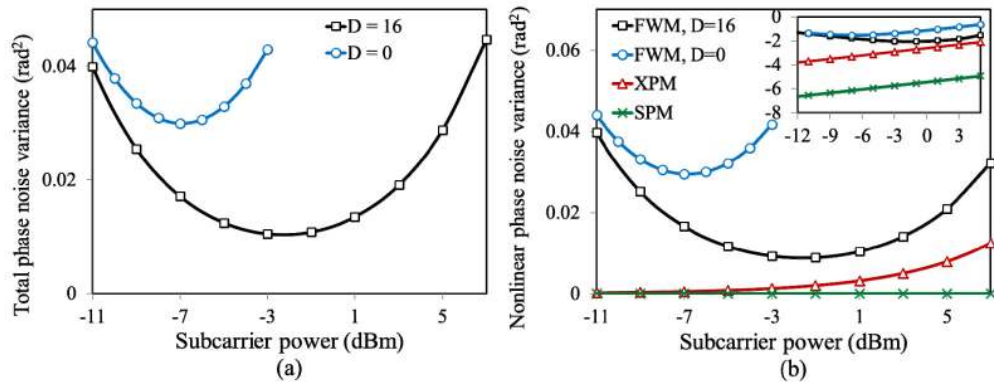

Fig. 3. Phase noise variance versus sub-carrier peak power for an all-optical OFDM system employing 4-QAM modulation format: (a) total phase noise variance; (b) phase noise variances due to SPM, XPM, FWM (at D = 0 ps/nm/km), and FWM (at D = 16 ps/nm/km).

Similar observations can be made for a 16-QAM all-optical OFDM system as depicted in Fig. 4. At fixed fiber length of 165 km (3 span), if D = 0 ps/nm/km and the launched power increases beyond −6 dBm, the phase noise variance would increase as shown in Figs. 4(a) and 4(b). By increasing the dispersion to D = 16 ps/nm/km, the degradation due to nonlinearity decreases and the minimum phase noise variance is obtained at a subcarrier power of −1 dBm.

The optimum launch power for 16QAM is higher than that for 4QAM because the 16QAM OFDM signal is transmitted over fiber length of 165 km while the transmission distance of the 4QAM OFDM system is 550 km. With longer transmission distance, the effect of phase noise on the transmitted signal become higher and the optimum power moves toward the lower power region. Further, Fig. 4(b) shows that the nonlinear phase noise due to the interaction of XPM and FWM with ASE noise becomes dominant at higher powers.

4.1.2. Phase noise variance versus number of subcarrier

Figures 5(a) and 5(b) shows the variance of phase noise due to the interaction of SPM, XPM, and FWM with ASE noise versus number of subcarriers for both 4-QAM and 16-QAM all-optical OFDM systems, respectively. For the 4-QAM system, the fiber length is 550 km (10 spans) long, the noise figure of optical amplifier is 6 dB, and the sub-carrier peak power is −3 dBm. For the 16-QAM system, the fiber length is 165 km (3 spans) and the sub-carrier peak power is −1 dBm. For the sake of convenience, the logarithmic values of phase variances versus the number of subcarriers are depicted in the inset of Fig. 5. As expected from Eq. (11), the SPM phase variance is robust against the number of subcarrier. On the other hand and in agreement with Eq. (11) and Eq. (17), by increasing the number of subcarriers, an increase in phase variation can be observed in both XPM and FWM respective nonlinearities. In the case of zero dispersion (D = 0 ps/nm/km), FWM nonlinear phenomenon is maximized where appropriate phase-matching condition is satisfied. This is due to the fact that the subcarriers of all-optical OFDM systems are derived from the same laser source and interact in a coherent manner. By increasing the dispersion to D = 16 ps/nm/km, the phase mismatch due to dispersion leads to a significant decrease of FWM phase variance.
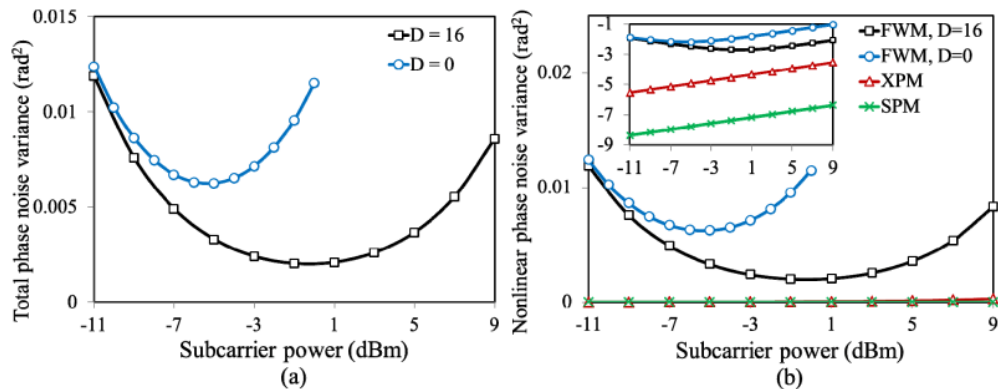

Fig. 4. Phase noise variance versus sub-carrier peak power for an all-optical OFDM system employing 16-QAM modulation format: (a) total phase noise variance; (b) phase noise variances due to SPM, XPM, and FWM.
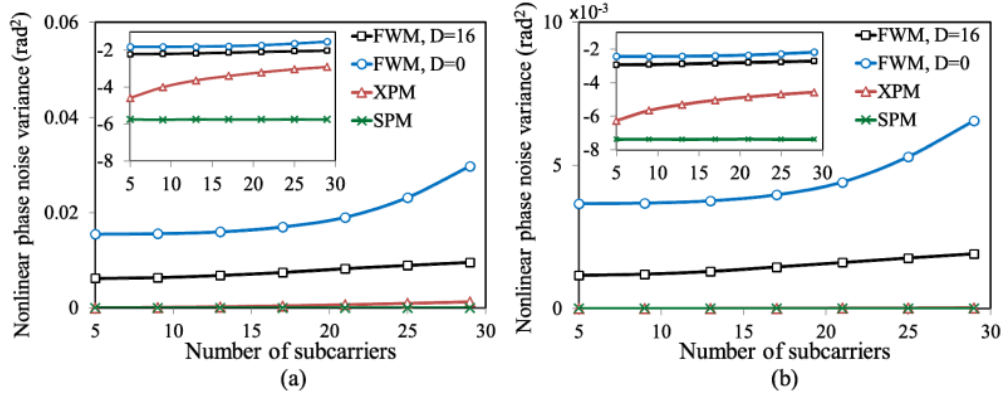
Fig. 5. Phase noise variance due to SPM, XPM, and FWM versus the number of subcarriers: (a) 4-QAM all-optical OFDM system; the inset is a logarithmic scale figure. (b) 16-QAM all-optical OFDM system; the inset is a logarithmic scale figure.

4.1.3. Phase noise variance versus fiber length

Figures 6(a) and 6(b) show the variance of the nonlinear phase noise as a function of the propagation distance for both 4- and 16-QAM all-optical OFDM systems, respectively. The number of subcarriers is fixed at 29. The subcarrier peak power is fixed at −3 dB for the 4-QAM system and −1 dBm for the 16-QAM system. During the simulation, the length of fiber span is fixed at 55 km and the number of spans is changed. As expected from Figs. 6(a) and 6(b), with large number of subcarriers, the nonlinear phase noise induced by FWM is significantly larger than that induced by either SPM or XPM. Moderate phase variation changes can be observed for SPM and XPM, rather than the FWM effect. This is because the overall interaction is dependent on the relative phases of all subcarriers in FWM.

To explain the effect of fiber span length on the phase noise, Figs. 6(c) and 6(d) compares between the nonlinear phase noise variances due to FWM and XPM for span lengths of 55 km and 80 km. It can be observed that the FWM effect for 80 km fiber span is higher than its effect for 55 km, while the XPM effect for 80 km is less than its effect for 55 km. At transmission distance of 550 km, ten fiber spans with length 55 km are required, while seven fiber spans with length 80 km are required to achieve 560 km. In other words, the number of optical amplifiers is reduced from 10 to 7 amplifiers. However, for span length of 80 km, the gain of amplifiers is higher and it adds more ASE noise. The interaction of ASE noise with FWM over longer fiber produces higher phase noise because FWM effect can efficiently accumulate over longer distances and add fluctuation to the transmitted signal. On other hand, XPM effect is more affected by the number of amplifiers rather than fiber length because its effect only changes the phase of optical signal. However, the nonlinear phase noise induced by FWM remains larger than that induced by XPM in 80 km and 55 km fiber span length.
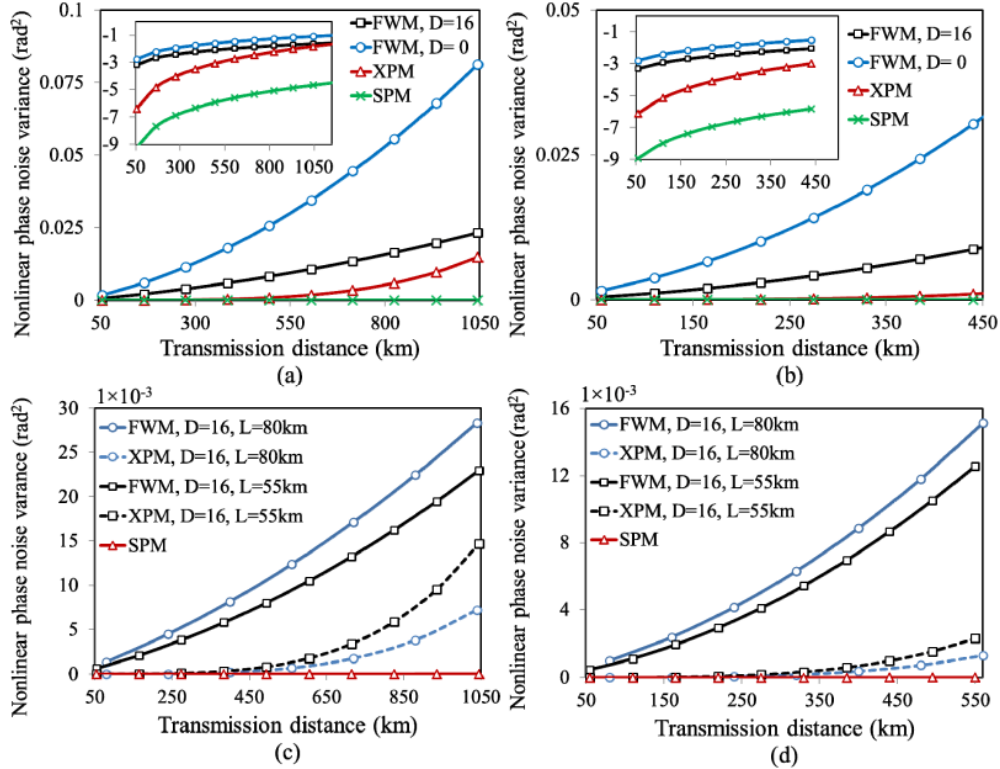
Fig. 6. Phase noise variance due to SPM, XPM, and FWM versus transmission distance: (a) 4-QAM all-optical OFDM system; the inset is a logarithmic scale figure. (b) 16-QAM all-optical OFDM system; the inset is a logarithmic scale figure. (c) 4-QAM all-optical OFDM system for span lengths 55km and 80km. d) 16-QAM all-optical OFDM system for span lengths 55km and 80km.

4.1.4. Phase noise variance versus symbol rate

The impact of the symbol rate on the total phase noise variance for both 4- and 16-QAM all-optical OFDM systems is investigated in this subsection. In Fig. 7, blue solid lines with hollow circle show the analytical results for a transmission fiber with D = 0 ps/nm/km, while black solid lines with hollow square show the analytical results with D = 16 ps/nm/km. It can be seen from the figures that there is minor change in the variance of the total phase noise by increasing the symbol rate for a fiber with D = 0 ps/nm/km. While for transmission fiber with D = 16 ps/nm/km, the phase variance decreases by increasing the symbol rate. This can be explained by phase mismatch definition $\beta_2 \Omega^2 z / 2$. As expected, for a fiber with D = 0 ps/nm/km, the effect of phase mismatch is zero. Therefore, high and constant FWM phase noise in all symbol rate ranges can be observed. On the other hand for the fiber with D = 16 ps/nm/km, the phase mismatch is higher than zero and its magnitude depends on the symbol rate. We observe that the magnitude of the FWM decreases when increasing the phase mismatch, which leads to low total phase noise at high symbol rate values.
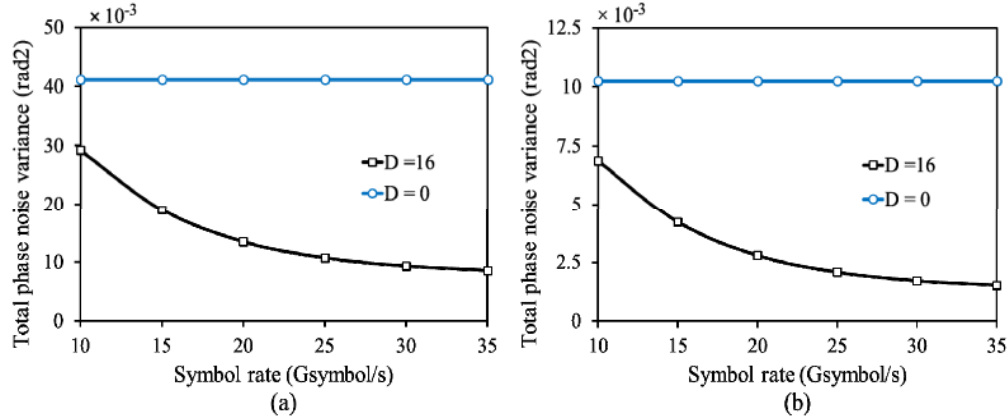
Fig. 7. Total phase noise variance versus symbol rate: (a) 4-QAM all-optical OFDM system. (b) 16-QAM all-optical OFDM system.

4.1.5. Phase noise variance versus subcarrier index

In this subsection, the effects of phase noise on the center frequency are investigated. It has been shown that the power density of FWM noise is higher in the center of the OFDM band than at the edge [17, 32]. In addition, the contributions of different subcarriers to the FWM noise, in general, are different. As a result, the power of the FWM noise depends strongly on the power distribution among the all-optical OFDM subcarriers. Figures 8(a) and 8(b) show the total nonlinear phase noise variance for each subcarrier for 4- and 16-QAM all-optical OFDM systems, respectively. Again, the 4-QAM-OFDM signal is transmitted over a distance of 550km (10 spans), while 16-QAM-OFDM signal is transmitted over 165 km (3 spans). It can be seen that the center subcarriers have a much larger contribution to the phase noise when compared with subcarriers at the edges for both SSMF (with D = 0 ps/nm/km) and zero dispersion fiber with D = 16 ps/nm/km.

4.2. Comparison of simulation and analytical results

In order to verify the accuracy of our analytical results, the error vector magnitude (EVM) for both analytical and simulation results are compared in this section. Furthermore, the effects of subcarrier's power and symbol rate on EVM are analyzed and explained. To estimate the nonlinear phase noise only, we set the laser phase noise to zero in our simulation.

4.2.1. EVM versus subcarrier peak power

In Fig. 9(a) and 9(b), we show the impact of subcarrier power on the EVM for both 4- and 16-QAM all optical OFDM systems, respectively. The transmission distances of 4- and 16-QAM systems are 550 km (10 spans) and 165 km (3 spans), respectively. The number of subcarriers and symbol rate are fixed at 29 subcarriers and 25 Gsymbol/s, respectively. In comparison with the phase noise variance (cf. Figure 4), same trend can be observed in EVM versus subcarrier peak power of Fig. 9. This is explained in [33], where for QAM systems with coherent detection, one would obtain the EVM as a function of the phase noise variance (σ^2) as:

$$EVM = \sqrt{\frac{1}{SNR} + 2 - 2\exp\left(\frac{-\sigma^2}{2}\right)},\qquad(18)$$

where, SNR is the signal noise ratio and the phase noise distribution is assumed to be Gaussian. In total agreement with the analytical results for 4-QAM all-optical OFDM system in the absence of dispersion, the EVM initially decreases up to 0.167 (corresponding to

launch power of −7 dBm). That is, the phase noise is the dominant at low launch power due to the interaction of ASE. However, as the launch power increases beyond −7 dBm, the EVM dramatically increases since the nonlinear phase noise due to the interaction of XPM and FWM with ASE noise becomes dominant at higher powers. At large dispersion values (D = 16 ps/nm/km), the EVM decreases to 0.11 when the subcarrier power reaches −3 dBm, beyond which; the magnitude of the EVM increases. Similarly, for 16-QAM all-optical OFDM system with D = 0 ps/nm/km, the EVM increases as the launched power increases beyond −6 dBm. For normal SMF fiber (D = 16 ps/nm/km), the EVM increases for values of subcarrier power higher than −1 dBm. Presented analytical results show good agreement with simulation results.
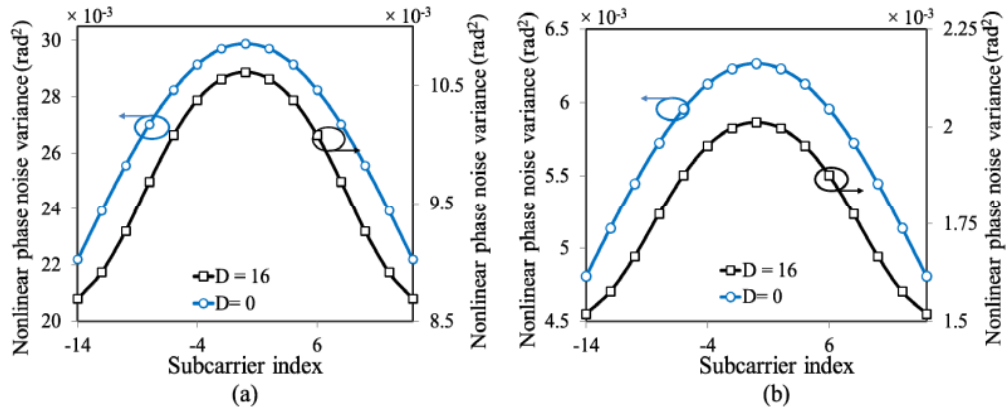

Fig. 8. Total phase noise variance versus subcarrier index: (a) 4-QAM all-optical OFDM system, (b) 16-QAM all-optical OFDM system.
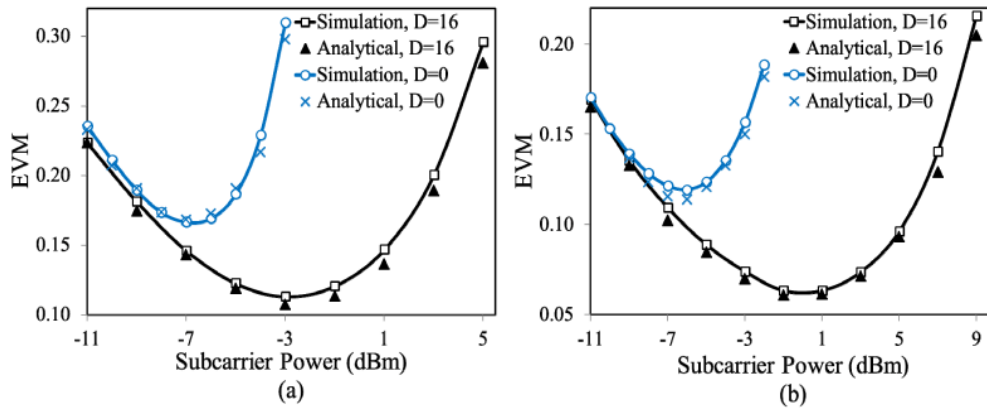

Fig. 9. EVM versus subcarrier power: (a) 4-QAM all-optical OFDM system. (b) 16-QAM all-optical OFDM system.

4.2.2. EVM versus symbol rate

Finally, Figs. 10(a) and 10(b) show the magnitude of EVM as a function of symbol rate for 4- and 16-QAM all-optical OFDM systems respectively. In agreement with our phase noise analytical results (cf. Figure 7), for the fiber with D = 16 ps/nm/km, the EVM decreases with the increase in the symbol rate, while the EVM approximately remains constant with increasing symbol rate for the fiber when D = 0 ps/nm/km. This can be explained by phase mismatch definition $\beta_2 \Omega^2 z / 2$. At D = 0 ps/nm/km, high and constant FWM phase noise in

all symbol rate ranges are observed as the phase mismatch equals zero. On the other hand, for the fiber with D = 16 ps/nm/km, the phase mismatch becomes higher as the phase mismatch between subcarriers totally depends on the symbol rate.
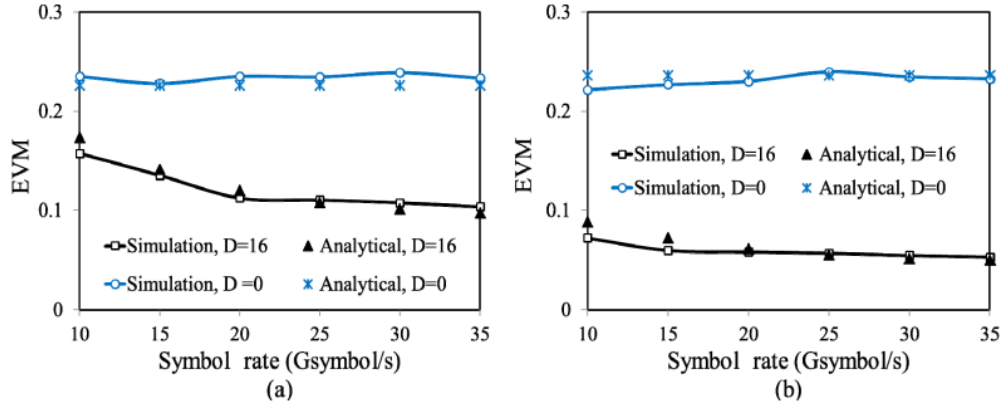

Fig. 10. EVM versus subcarrier power: (a) 4-QAM all-optical OFDM system. (b) 16-QAM all-optical OFDM system.

Finally yet important, our analytical model is also valid for higher-level modulation format such as mPSK and mQAM system over 64-level. For example, when the subcarriers are modulated by 4QAM format, the $u(0,t)$ is defined with $a_k \in \{-1,1\}$ and $b_k \in \{-1,1\}$, while the $u(0,t)$ is described with $a_k \in \{-3,-1,1,3\}$ and $b_k \in \{-3,-1,1,3\}$ for 16QAM format. In case of mPSK or mQAM system over 64-level, the a_k and b_k are defined in analytical model according to its corresponding constellation.

5. Conclusion

Analytical equations for nonlinear phase variances, due to the interaction of SPM, XPM, and FWM with ASE noise in both 4- and 16-QAM all optical OFDM systems are derived. The effects of the number of subcarriers, fiber length, subcarrier peak power, and dispersion on the nonlinear phase noise are investigated in a quantitative manner. It is found that the nonlinear phase noise induced by FWM is the dominant nonlinear effect in all-optical OFDM systems. This is because the interaction is dependent on the relative phases of all subcarriers in FWM, where appropriate phase-matching conditions from same laser source are always satisfied at zero dispersion (D = 0 ps/nm/km). When increasing the dispersion (D = 16 ps/nm/km), the phase mismatch due to dispersion would compensate the FWM phase variation. In 4-QAM all-optical OFDM systems, the point of optimum performance is achieved at −3 dBm when the standard single mode optical fiber (SSMF) is employed. This point of optimum performance increases to −1 dBm for the case of 16-QAM all-optical OFDM systems. In addition, the accuracy of our analytical model has been verified by quantifying the error vector magnitude (EVM) using both simulation and analytical models. It turned out that both EVM results are in good agreement with each other.